Volume 54(5): 525–537, 2006
Journal of Histochemistry & Cytochemistry
http://www.jhc.org

ARTICLE

Fibromodulin-deficient Mice Display Impaired Collagen Fibrillogenesis in Predentin as Well as Altered Dentin Mineralization and Enamel Formation

Michel Goldberg, Dominique Septier, Åke Oldberg, Marian F. Young, and Laurent G. Ameye

Laboratoire Réparation et Remodelage des Tissus Oro-Faciaux, EA 4296, Groupe Matrices extracellulaires et biominéralisations, Faculté de Chirurgie Dentaire, Université Paris V, Montrouge, France (MG,DS); Lund University, Lund, Sweden (AO); National Institute of Dental and Craniofacial Research, National Institutes of Health, Bethesda, Maryland (MFY,LGA); and Nestlé Research Center, Lausanne, Switzerland (LGA)

SUMMARY To determine the functions of fibromodulin (Fmod), a small leucine-rich keratan sulfate proteoglycan in tooth formation, we investigated the distribution of Fmod in dental tissues by immunohistochemistry and characterized the dental phenotype of 1-day-old Fmod-deficient mice using light and transmission electron microscopy. Immunohistochemistry was also used to compare the relative protein expression of dentin sialoprotein (DSP), dentin matrix protein-1 (DMP 1), bone sialoprotein (BSP), and osteopontin (OPN) between Fmod-deficient mice and wild-type mice. In normal mice and rats, Fmod immunostaining was mostly detected in the distal cell bodies of odontoblasts and in the stratum intermedium and was weaker in odontoblast processes and predentin. The absence of Fmod impaired dentin mineralization, increased the diameter of the collagen fibrils throughout the whole predentin, and delayed enamel formation. Immunohistochemistry provides evidence for compensatory mechanisms in Fmod-deficient mice. Staining for DSP and OPN was decreased in molars, whereas DMP 1 and BSP were enhanced. In the incisors, labeling for DSP, DMP 1, and BSP was strongly increased in the pulp and odontoblasts, whereas OPN staining was decreased. Positive staining was also seen for DMP 1 and BSP in secretory ameloblasts. Together these studies indicate that Fmod restricts collagen fibrillogenesis in predentin while promoting dentin mineralization and the early stages of enamel formation.

(J Histochem Cytochem 54:525–537, 2006)

KEY WORDS
fibromodulin
dentin
enamel
dentin sialoprotein
dentin matrix protein 1
bone sialoprotein
osteopontin
tooth phenotype

SMALL LEUCINE-RICH PROTEOGLYCANS (SLRPs) are important constituents of dental tissues (Goldberg and Takagi 1993; Linde and Goldberg 1993; Steinfort et al. 1994; Lormée et al. 1996; Embery et al. 2001). Class I SLRPs include decorin and biglycan, both of which bear one or two chondroitin/dermatan sulfate glycosaminoglycan (CS/DS GAG) chains. Class II SLRPs include lumican, fibromodulin (Fmod), and osteoadherin, all of which bear keratan sulfate (KS) GAG chains (Iozzo 1997, 1999; Neame and Kay 2000). GAGs and proteoglycans (PGs) display specific distribution in dental tissues (Takagi et al. 1990; Septier et al. 1998; Hall et al. 1999). The presence, distribution, and function of decorin and biglycan in dental tissues have been extensively studied in the past few years (Septier et al. 2001; Goldberg et al. 2002,2003,2005). Biglycan and decorin have recently been shown to contribute to tooth development. Biglycan represses amelogenin expression and enamel formation, whereas decorin promotes dentin mineralization (Goldberg et al. 2002,2005). Whereas functions of Class I SLRPs in tooth formation are beginning to be deciphered, the functions of Class II SLRPs are still far from clear (Hall et al. 1999; Buchaille et al. 2000). In predentin, KS and lumican display a positive gradient of accumulation from the proximal to the distal part of predentin. This uneven distribution suggests a role for KS GAGs and PGs in the mineralization process (Hall et al. 1999; Goldberg et al. 2003). Presently, very little information is available about Fmod. During mouse development, Fmod mRNA was detected in the outer enamel epithelium (as well as

Correspondence to: Michel Goldberg, Faculté de Chirurgie Dentaire, Université Paris V 1, rue Maurice Arnoux, 92120 Montrouge, France. E-mail: mgoldod@aol.com

Received for publication February 13, 2005; accepted November 16, 2005 [DOI: 10.1369/jhc.5A6650.2005].

0022-1554/05/$3.30

in bone ossification centers and maturing cartilage) but not in the dental papilla (Wilda et al. 2000).

Fmod was originally identified in cartilage, tendon, skin, sclera, and cornea as a 59-kDa protein. The leucine-rich protein (42 kDa) is substituted by one KS chain and oligosaccharides (Oldberg et al. 1989). Its molecular weight varies with age, tissue, and species (Ezura et al. 2000). Fmod is a latent TGFβ modulator during skin development and wound healing (Soo et al. 2000). In addition, like other SLRPs, it is most probably implicated in the lateral aggregation of collagen fibrils that orient fibrillogenesis (Scott 1988,1996; Milan et al. 2005). Fmod and lumican bind to the same region on collagen type I fibrils (Svensson et al. 2000). Some reports suggest that decorin and Fmod inhibit the lateral aggregation of collagen fibrils (Vogel and Trotter 1987; Scott 1988; Scott and Parry 1992; Font et al. 1998; Matheson et al. 2005), although most morphometric analyses published so far demonstrate that, in tendon, Fmod-deficient mice have thinner collagen fibrils than wild-type (WT) animals (Svensson et al. 1999; Ezura et al. 2000; Ameye et al. 2002; Chakravarti et al. 2003). Through its ability to control collagen fibrillogenesis, Fmod could modulate mineralization.

In the present investigation, we aimed to study the potential functions of Fmod in dental tissue formation and mineralization. To do so, we investigated first the distribution of Fmod in the first molar of 1-day-old WT mice. Second, we compared the morphology and ultrastructure of molars and incisors from 1-day-old WT and Fmod-deficient mice. Third, we studied by postembedding electron-immunogold labeling the distribution of Fmod in the various cellular and extracellular compartments of the forming part of the incisor. Finally, to evaluate the overall consequences of the absence of Fmod on the composition of dental tissues, the distribution and levels of labeling of amelogenin and of four SIBLINGS (Small Integrin-Binding Ligand N-linked Glycoproteins) were compared by immunohistochemistry in 1-day-old WT and Fmod-deficient mice. The SIBLINGs selected for immunostaining were the major phosphorylated extracellular proteins known to be implicated in dentin and bone biomineralization: DSP, DMP 1, BSP, and OPN (Fisher and Fedarko 2003), although these molecules have also been identified in non-mineralized tissues (Fisher et al. 2004; Ogbureke and Fisher 2004,2005).

Materials and Methods

Production of LF-150 Rabbit Antiserum to Mouse Fmod

Two peptides corresponding to 39D–58E and 144D–159R of mouse Fmod (Swissprot accession #P50608) were synthesized with an additional cysteine on each amino termini. The peptides were conjugated through their cysteine to activate keyhole limpet hemocyanin (Pierce; Rockford, IL) and injected as four boosts into a New Zealand White rabbit at an American Association for Accreditation of Laboratory Animal Care-approved facility (Covance; Denver, PA) under approved animal protocol.

Generation and Genotyping of Fmod-deficient Mice

All experiments were performed under an institutionally approved protocol for the use of animals in research (#NIDCR-IRP-98-058 and 01-151). Fmod-deficient mice were generated by gene targeting in embryonic stem cells (Svensson et al. 1999) and bred for several generations to C3H females. All mice were genotyped by PCR analysis using DNA isolated from a small tail biopsy as previously described (Ameye et al. 2002). PCR products were resolved by electrophoresis through 1.8% agarose gels yielding bands of 280 bp for WT Fmod allele and 603 bp for targeted Fmod allele.

Light and Transmission Electron Microscopy

Six C3H Fmod-deficient mice were sacrificed at day 1 after birth, and mandibles were prepared for light microscopy. Tissues from six C3H WT age-matched mice were processed simultaneously as controls. Mandibles were dissected and immersed in 4% paraformaldehyde and buffered with 0.1 M sodium cacodylate, pH 7.2–7.4, for 24 hr at 4C. After several rinses in cacodylate buffer, undemineralized mandibles were dehydrated in graded ethanols and embedded in Paraplast (Oxford; St. Louis, MO). Serially cut transverse 5- to 7-μm-thick sections were used for morphological and immunohistochemical observations.

Six other mice per group (WT and Fmod-deficient mice) were used for electron microscopy. Twelve mandibles per group were reduced in size with a razor blade and sliced transversally into segments containing the molars and the subjacent incisor. Segments were immersed in a fixative solution containing 1% glutaraldehyde, buffered with 0.1 M sodium cacodylate, pH 7.2–7.4, for 1 hr at 4C, and then immersed overnight in 0.2 M cacodylate buffer. They were postfixed with 2% osmium tetroxide in the same buffer for 30 min at room temperature (RT). After dehydration in graded ethanols, segments were embedded in Epon.

Semithin sections were stained with toluidine blue. Ultrathin sections were stained with uranyl acetate and lead citrate and examined with a Jeol 100B transmission electron microscope (Jeol; Tokyo, Japan) operating at 80 kV.

Calculations of the mean diameter of collagen fibrils were carried out on sections from 12 mandibular incisors per group. Predentin was divided arbitrarily into halves, an inner zone and an outer zone. Six to nine electron micrographs per tooth, enlarged at a final magnification of ×54,000, were taken systematically in each zone, and the diameters of 1800–2000 collagen fibrils per group (at least 900 fibrils per zone) were measured with a glass magnifier equipped with a reticule allowing scoring at a 0.1-mm level. Measurements were pooled according to the genotype and the zone. Mean values and standard deviations were calculated. For fibril density, the same micrographs were used and the number of fibrils per μm^2 was calculated from the number of fibrils present in small square areas (2×2 mm). Similarly, this was carried out for the 12 teeth of the six mice of each group. Data were analyzed by Student's *t*-test; $p \leq 0.05$ was considered statistically significant.

Immunohistochemistry

Mandibles obtained from six WT and six Fmod-deficient mice were dissected, reduced in size, and immersed in 4% paraformaldehyde buffered with 0.1 M sodium cacodylate, pH 7.2–7.4, for 24 hr at 4C. After several rinses in cacodylate buffer, undemineralized mandibles were dehydrated in graded ethanols and embedded in Paraplast (Oxford). Five- to seven-µm-thick sections were treated in methanol to inhibit endogenous peroxidases. Sections were saturated at 4C overnight with PBS-BSA 1% and incubated in the primary antibody for 2 hr at RT. In a pilot study, we first tested the distribution of the labeling in the mandible, and we did not detect any differences between keratinase-digested sections and sections not digested by the enzyme prior to staining. Second, sharpness of the staining was slightly decreased in keratanase-treated sections; therefore, the sections examined here were not pretreated by the enzyme. In addition to the anti-Fmod, we also investigated the labeling obtained with antibodies raised against decorin, biglycan, amelogenin, and four SIBLINGs: DSP, DMP 1, BSP, and OPN. Table 1 indicates the origin of the primary antibody and its concentration.

Treatment with the primary antibody was followed by incubation with the secondary antibody, a peroxidase-conjugated goat anti-mouse IgG (Dako A/S; Glostrup, Denmark). Immunoreactivity was detected with diaminobenzidine diluted with PBS. We labeled nine sections (three slides) per antibody and per group of mice. Two examiners evaluated the staining density independently, and some differences in the evaluation were discussed. Staining was scored as very strong (+++), strong (++), weak (+), more or less detectable with some variations between sections (±), or unlabeled (−).

Controls were carried out by absorption using the antibody with the protein at appropriate concentrations and also by omitting the primary antibody. The nature of the molecules in the tooth germs and the specificity of the antibodies used were confirmed by Western blots.

Electron-Immunogold Labeling

Due to the distance between laboratories and to technical constraints, it was not possible to embed mice mandibles in low temperature Lowicryl K4M. As an alternative, we chose to investigate the postembedding immunogold labeling after preliminary light microscopy immunostaining had confirmed that the staining pattern for Fmod in mandibles from WT mice and rats was very similar (data not shown).

Sprague Dawley male rats (100 g body weight) were anesthetized with an injection of chloral hydrate and were then perfused intracardially with a solution containing 1% glutaraldehyde buffered with 0.1 M sodium cacodylate, pH 7.2–7.4. After 10 min, the two mandibular incisors and the surrounding tissues were dissected out. Segments from the forming part of the incisor (the first 6 mm) were sliced with a razor blade into segments ~2 mm thick. Segments were immersed in the fixative solution for 1 hr at 4C and then immersed overnight in 0.2 M cacodylate buffer. After dehydration in graded ethanols, segments were embedded in Lowicryl K4M and polymerized at −20C with UV light.

Ultrathin sections incubated in PBS-5% BSA at RT for 90 min were incubated with the primary antibody (1/150 dilution) for 2 hr at RT. After three rinses with PBS-1% BSA, sections were incubated with a 1:100 dilution of the secondary antibody, a goat anti-rabbit IgG coupled to 15-nm colloidal gold (Auroprobe GAR IgG-G15; Amersham, Poole, UK) for 90 min at RT. Sections were rinsed in PBS and stained with uranyl acetate for 5 min and then with lead citrate for 1 min. They were examined with a Jeol 100B electron microscope operating at 80 kV. Controls were performed by omitting or substituting the primary antiserum with non-immune serum.

Labeling densities in each morphological compartment were obtained by counting the number of gold–antibody conjugates in 40- to 90-4-cm^2 areas (2 × 2 cm) on electron micrographs enlarged to a final magnification of ×54,000. Labeling densities were expressed as the number of gold particles per µm^2 followed by the SE of the mean. Background labeling was scored in the lumen of pulp vessels and in lateral parts of the sections where no biological material was present. Statistical comparison between two mean values was carried out using Student's *t*-test; p values ≤ 0.05 were considered significant.

Results

Fmod Distribution in Teeth

To investigate Fmod distribution in teeth, a mouse Fmod antiserum was produced. By Western blot, this antibody reacted strongly with a single 53-kDa band in

Table 1 Origin of the antibodies used and concentration at which they were diluted[a]

Antibody	Origin	Concentration
Anti-fibromodulin (anti-Fmod)	LF 150 (Larry Fisher, NIH, Bethesda, MD)	1:100
Anti-amelogenin	Biora (generous gift from Peter Lyngstadaas, Biora, Malmoe, Sweden)	1:50
Anti-dentin sialoprotein (anti-DSP)	LF 153 (Larry Fisher, NIH)	1:100
	or polyclonal rabbit anti-SP (generous gift from WT Butler; Houston, TX)	1:200 + secondary antibody: swine anti-rabbit (Dako; Glostrup, Denmark)
Anti-dentin matrix protein 1 (anti-DMP-1)	LF 143 (Larry Fisher, NIH)	1:100
Anti-bone sialoprotein (anti-BSP)	LF 100 (Larry Fisher, NIH)	1:100
Anti-osteopontin (anti-OPN)	LF 123 (Larry Fisher, NIH)	1:100
Anti-biglycan (anti-BGN)	LF 107 (Larry Fisher, NIH)	1:100
Anti-decorin (anti-DCN)	LF-113 (Larry Fisher, NIH)	1:100

[a]Details about the SLRP and SIBLING antibodies may be found in Fisher et al. (1995).

keratanase-treated extracts of first mandibular tooth germs from newborn mice (Figure 1A). Specificity of the antiserum toward Fmod was shown by the absence of any cross-reactivity in similar extracts from Fmod-deficient mice. Specificity was further confirmed by the absence of signal in tooth sections from Fmod-deficient mice by immunochemistry (Figure 1B).

Using this antiserum in WT molars at day 1, Fmod was detected in the distal part of the cell bodies of the secretory odontoblasts, mostly along the distal terminal junctional complex (Figures 1C and 1D). In some sections, odontoblast processes were also stained (Figure 1D). Fmod was also expressed in the enamel organ along the stratum intermedium (SI) with local

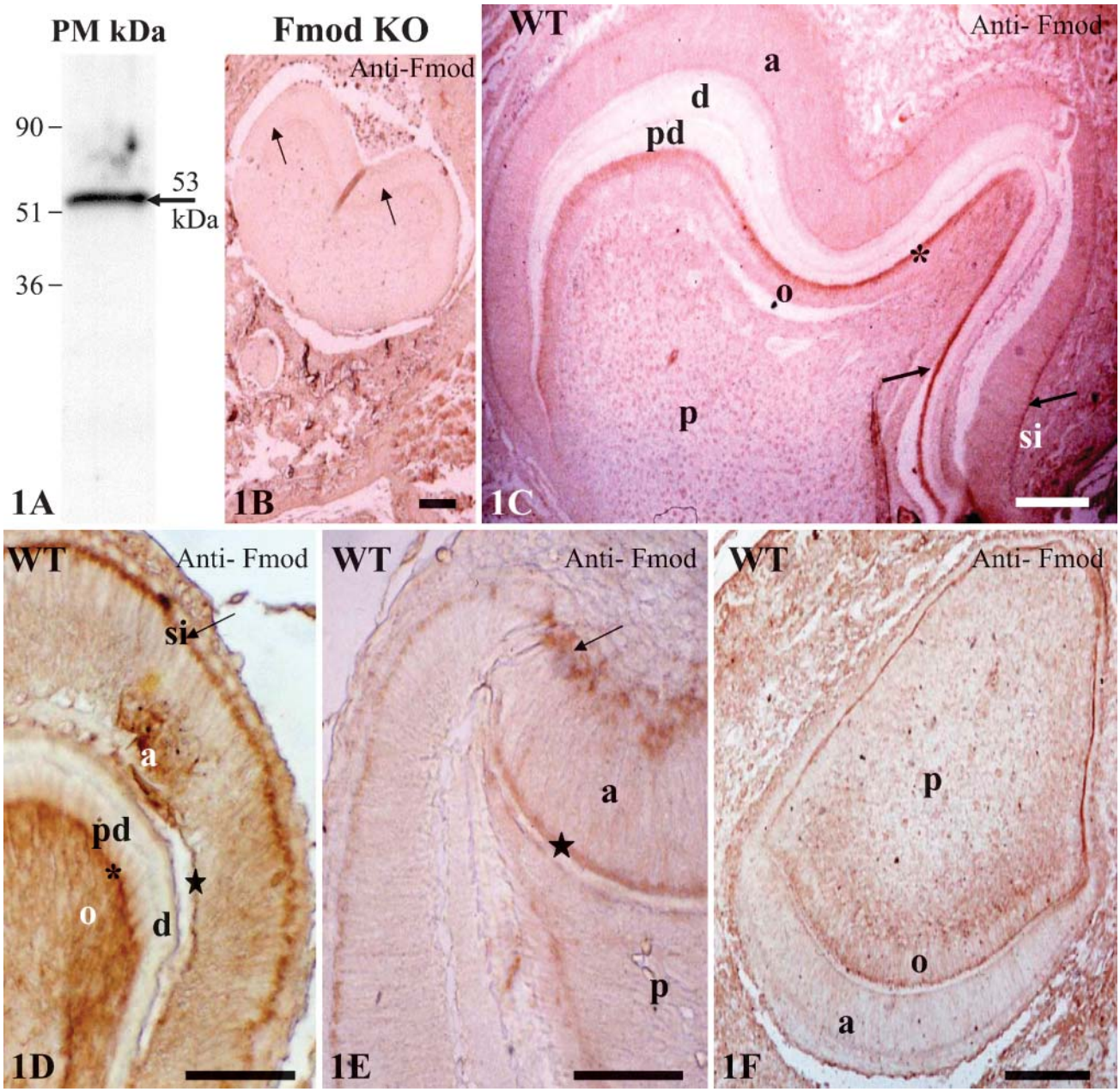

Figure 1 Fibromodulin (Fmod) expression in dental tissues. (**A**) Fmod Western blot of an extract of first molar tooth germs from newborn mouse. A single band is detected with a MW of 53 kDa. (**B**) Mandibular molar from a Fmod-deficient mouse (Fmod KO). No anti-Fmod staining is detectable in the molar (arrow). (**C–E**) Molars of newborn wild-type (WT) mice. Staining is mostly seen at the distal border of odontoblasts (o) along the junctional complex (asterisk) and in the stratum intermedium (si). a, ameloblasts, pd, predentin; d, dentin; p, pulp. (**F**) Incisor of newborn WT mouse. The same staining pattern as in molar is observed. Bars: **B** = 50 μm; **C–F** = 100 μm.

variations in staining intensity (Figures 1D and 1E). In some sections, Fmod was expressed in the distal terminal border of ameloblasts located in enamel-free areas at the tip of cusps (Figure 1E). No extracellular labeling was detected with the light microscope, and predentin, dentin, and forming enamel were unstained (Figures 1C–1E). The same distribution was seen in the incisors together with a faint staining of the subodontoblastic cell layer (Figure 1F). It is possible that in the absence of keratinase treatment, some signal for Fmod was blocked. Nevertheless, high levels of immunoreactivity indicate a strong and selective intracellular expression indicating that, under the conditions used, Fmod can be detected.

Upon examination of the samples with the electron microscope, the highest labeling densities were obtained in the SI, confirming the light microscope data obtained in mice dental tissues and in odontoblast cell bodies (Table 2). Labeling was weaker in secretory ameloblast cell bodies and was further decreased in odontoblast and ameloblast cell processes. In contrast to the distribution observed with the light microscope, some labeling was also seen in extracellular compartments. The outer part of the forming enamel was labeled, and a clear homogeneously distributed labeling was also seen throughout the predentin with immunogold complexes always closely associated with the collagen fibrils (results not shown). The lowest densities, although still above the background labeling, were scored in dentin, with no statistically significant difference between the mantle dentin, the circumpulpal dentin, and the metadentin (the 0.5- to 2.5-μm-thick border located at the mineralization front (Goldberg and Septier 1996) (see Table 2).

Table 2 Number of Fmod antibody–colloidal gold complex per μm^2 in ultrathin sections of rat incisors (±SE of the mean)[a]

Compartment	Mean value/μm^2 ± SE
Stratum intermedium	11.9 ± 1.5
Ameloblast cell body	9.0 ± 1.1
Ameloblast Tomes' processes	6.1 ± 1.0
Forming enamel	6.4 ± 0.6
Mantle dentin	1.8 ± 0.8
Circumpulpal dentin	1.3 ± 0.5
Metadentin	1.4 ± 0.6
Predentin a: distal third	2.8 ± 0.7
Predentin b: central third	3.2 ± 0.6
Predentin c: proximal third	3.4 ± 1.0
Odontoblast processes	6.2 ± 1.0
Odontoblast cell bodies	12.2 ± 2.0
Background labeling	0.2 ± 0.3

[a]All values scored were statistically significantly above background labeling. In predentin, the density scored in the distal third (a) was reduced compared with the central (b) and proximal (c) thirds, but the differences were not statistically significant.

Comparative Histology and Ultrastructure of Molars from 1-Day-Old WT Mice and 1-Day-Old Fmod-deficient Mice

To directly investigate the in vivo function of Fmod during tooth formation, we compared the histology of teeth from 1-day-old WT and Fmod-deficient mice. In WT mandibles, first molars were not erupted with the germs still at the late bell stage (Figure 2A). The crowns were formed but not the root parts. The crown comprises an inner dental papilla covered by an outer enamel organ. Dental papilla was composed of a central embryonic pulp covered by a characteristic triple layer of an inner continuous layer of odontoblasts, an intermediate 15–20-μm thick predentin layer, and an outer layer of dentin. Dentin thickness was variable: thicker in the cusps, thinner in the lateral parts of the bell, and absent near the cervical zone at the rim of the bell. In the enamel organ near the tip of the cusps adjacent to dentin, a thin layer of forming enamel had been laid down by the ameloblasts (Figure 2B). The enamel organ ended at the rim of the bell where the Hertwig's sheath involved in root formation just started to be formed.

Histologically, Fmod deficiency did not seem to dramatically impair molar morphogenesis. In Fmod-deficient mice at day 1, histology of the first molar was almost identical to the WT situation (Figure 2C). The only noticeable difference was that in Fmod-deficient mice, the thickness of the forming enamel was reduced to half compared with WT (Figure 2D; Table 3).

To confirm this assumption, the ultrastructures of WT and Fmod-deficient molars at day 1 were compared. In WT, dentin was homogeneously electron dense (Figure 3A). In contrast, Fmod-deficient dentin had a heterogeneous appearance: electron-dense areas bordered small and large hypomineralized electron-lucent areas (Figure 3B). The mantle dentin near the dentino-enamel junction, which was >10-μm thick, also was hypomineralized (data not shown). At the border between predentin and dentin, metadentin was abnormally electron lucent, also indicating a defect in mineralization (Figures 3C and 3D). However, compared with WT, no significant variation in metadentin thickness was detectable (0.5 to 0.7 μm in WT vs 0.5 to 0.9 μm in absence of Fmod). This contrasts with the significant increase in metadentin thickness observed in the absence of biglycan or decorin, two other small leucine-rich proteoglycans (Goldberg et al. 2005). Diameter of the collagen fibrils of the whole predentin was significantly increased in the absence of Fmod compared with WT (Figure 4). No difference was found between the groups of mice with respect to fibril density per μm^2. At the dentino-enamel junction, aprismatic enamel formation occurred normally in the absence of Fmod although the enamel thickness was significantly decreased compared with WT in the molar as well as in the incisor (Table 3). Rodent inner enamel is composed

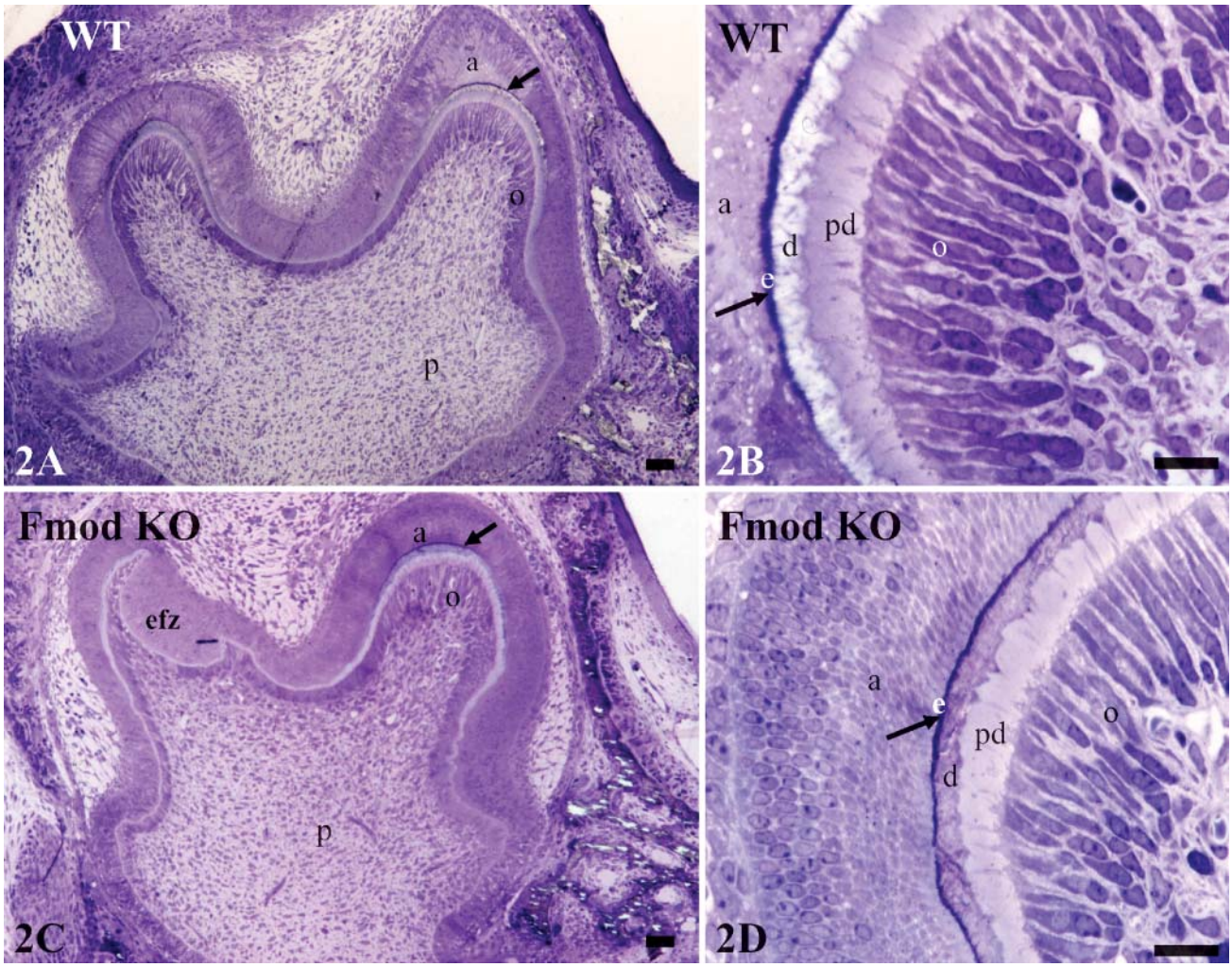

Figure 2 Histology of WT and Fmod KO molars. (**A,B**) WT mouse. (**C,D**) Fmod KO. Dentin is stained by toluidine blue in Fmod KO (**D**) but not in WT (Figure 1B). d, dentin, pd, predentin; e, early-forming enamel; efz, enamel-free zone; a, ameloblasts; o, odontoblasts; p, pulp. Bars: **A,C** = 50 μm; **B,D** = 20 μm.

first by an aprismatic border, followed by a prismatic enamel composed of rods and interrod material. In the forming part of the Fmod-deficient incisor, enamel was mostly formed by interrods with a delayed formation of the rods (data not shown). Together these observations clearly indicate that dentinogenesis and early stages of amelogenesis are impaired by the absence of Fmod.

Table 3 Thickness (in μm ± SEM) of dentin, predentin, and enamel in teeth from wild-type (WT) and Fmod-deficient mice[a]

	WT (a)	Fmod-deficient (b)
Predentin in molar	22.8 ± 0.9	18.8 ± 0.8 a vs b: ns
Dentin in molar	19.4 ± 0.8	20.2 ± 1.1 a vs b: ns
Enamel in molar	10.5 ± 0.8	5.8 ± 0.6 a vs b:***
Enamel in the forming part of the incisor	4.9 ± 0.6	3.3 ± 0.8 a vs b:*

[a]Thickness of dentin, predentin, and enamel was measured on five semithin Epon sections per tooth. Data were collected from the two first mandibular molars and the two mandibular incisors of three mice per group. Differences between WT and Fmod-deficient mice were statistically significant for enamel thickness.
*$p<0.05$.
***$p<0.001$. Absence of statistically significant difference in the predentin and dentin compartments suggests that the level of the sections matched.

Regulation of Expression of Extracellular Matrix Proteins in Absence of Fmod

To investigate the possible existence of compensatory mechanisms between Fmod and two other closely related small leucine-rich proteoglycans, decorin and biglycan, anti-decorin and anti-biglycan stainings were performed on WT and Fmod-deficient sections. No compensatory mechanism was detected. Intensities of stainings between WT and Fmod-deficient sections were similar (data not shown).

Because amelogenin is overexpressed in BGN-deficient mice (Goldberg et al. 2002,2005), sections of WT and Fmod-deficient mice were stained with

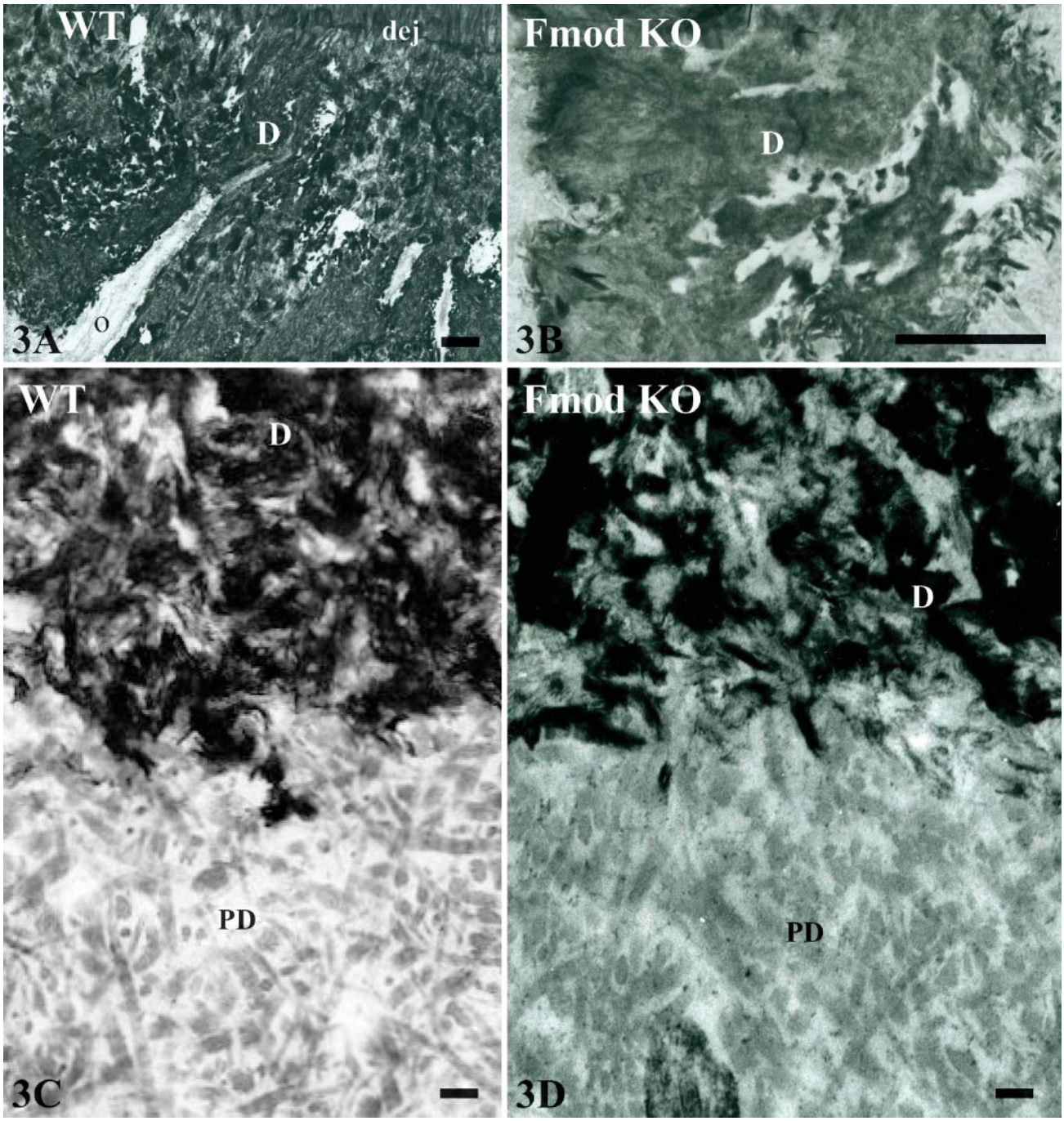

Figure 3 Ultrastructure of newborn WT mice and Fmod KO. (**A,C**) WT mice molar. (**B,D**) Fmod KO molar. (**A**) Normal dentin displaying tubule-like structures containing odontoblast processes. dej, dentino-enamel junction; o, odontoblasts. (**B**) Hypomineralized dentin (d); a, ameloblasts. (**C,D**) Predentin (PD) and dentin (D). Note the large electron-lucent areas in dentin in (**D**) compared with (**C**). Bars: **A,B** = 1 μm; **C,D** = 100 nm.

anti-amelogenin antibodies to determine if the absence of Fmod affected the protein expression of amelogenin. However, no major difference could be detected. In 1-day-old WT and Fmod-deficient teeth, immunoreactivity for amelogenin was restricted to the secretory ameloblasts and to the thin layer of forming enamel in molars and incisors (Figures 5A–5D).

Finally, sections from WT and Fmod-deficient mice were stained with antibodies raised against DSP, DMP 1, BSP, and OPN to determine if the labeling was affected by the absence of Fmod. In the molars, comparison between Fmod-deficient and WT mice showed a clear reduction of the staining intensity after DSP and OPN labeling (Figures 6A, 6B, 6M, and 6N; Table 4).

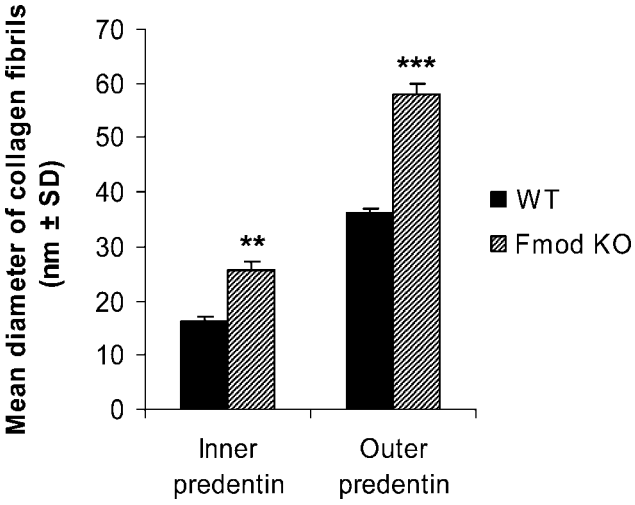

Figure 4 Comparison of the mean diameter of collagen fibrils in nanometers (mean ± SD) in inner and outer predentin of molars from newborn WT and Fmod KO. Data obtained from measurements carried out on 10 micrographs per tooth enlarged at a final magnification of ×54,000. Twelve molars from six mice per group were studied (two molars per animal). $^{**}p<0.01$; $^{***}p<0.001$.

In contrast, staining was enhanced for DMP 1 and BSP (Figures 6E, 6F, 6I, and 6J). In the incisor, compared with WT, staining of Fmod-deficient mice was clearly enhanced in the pulp and odontoblasts for DSP, DMP 1, and BSP but reduced after OPN staining (Figures 6C, 6D, 6G, 6H, 6K, 6L, 6O, and 6P; Table 4). Surprisingly, Fmod-deficient incisors displayed a strongly positive DMP 1 and BSP labeling in secretory ameloblasts (Figures 6H and 6L). Together these results indicate that the absence of Fmod induces molecule-specific compensatory mechanisms with some important differences between molars and incisors.

Discussion

To decipher the functions of Fmod in tooth formation, we characterized for the first time (1) the distribution of Fmod in teeth from 1-day-old mice with the light microscope and in a parallel study, the electron-immunogold staining of Fmod in the rat incisor, (2) the dental phenotype of 1-day-old Fmod-deficient mice, and (3) the consequences of Fmod deficiency on other extracellular matrix proteins. We report here that Fmod labeling is detected in the distal part of the cell bodies of secretory odontoblasts and ameloblasts, in the SI, and in predentin, and that Fmod deficiency increased the diameter of the collagen fibrils in predentin, resulting in hypomineralization of dentin. In addition, Fmod deficiency delayed enamel formation and affected the level and pattern of expression of OPN, DSP, DMP 1, and BSP but not those of biglycan, decorin, and amelogenin. Together these studies indicate that Fmod plays a central role in dentin and enamel formation even if the reported dental alterations did not seem to have a major functional impact as Fmod-deficient mice were able to eat normally even when adults.

Wilda et al. (2000) previously reported that the expression of Fmod during fetal development was restricted to the outer enamel epithelium. By comparison, our results indicate that, after birth, the immunostaining pattern of Fmod is much broader. In molars from newborn mice, Fmod antibody strongly labeled the odontoblasts and cells from the SI and, to a lesser ex-

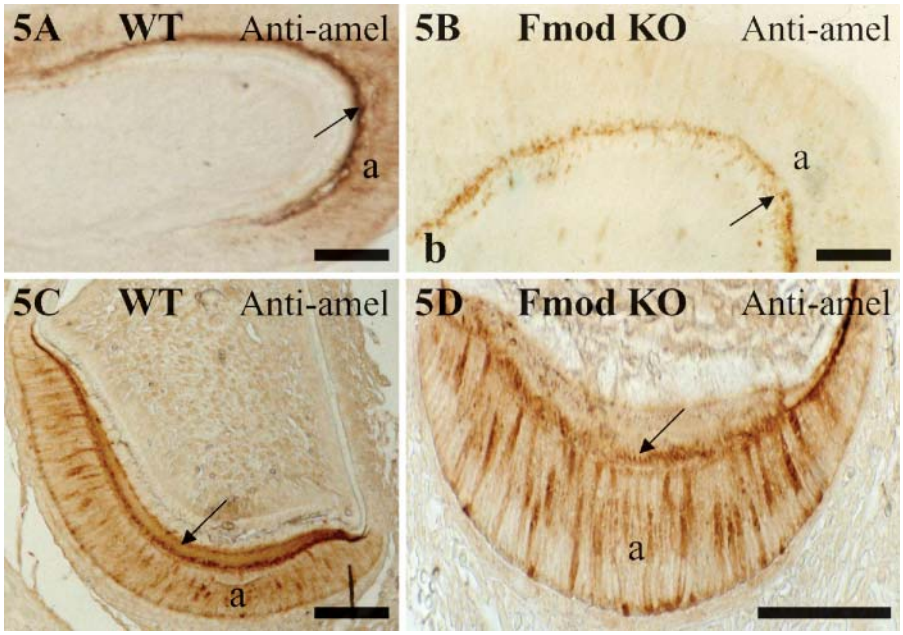

Figure 5 Amelogenin expression in molars (**A,B**) and incisors (**C,D**) from WT and Fmod KO. a, ameloblast. No major visible difference between the two groups was observed. Bar = 50 μm.

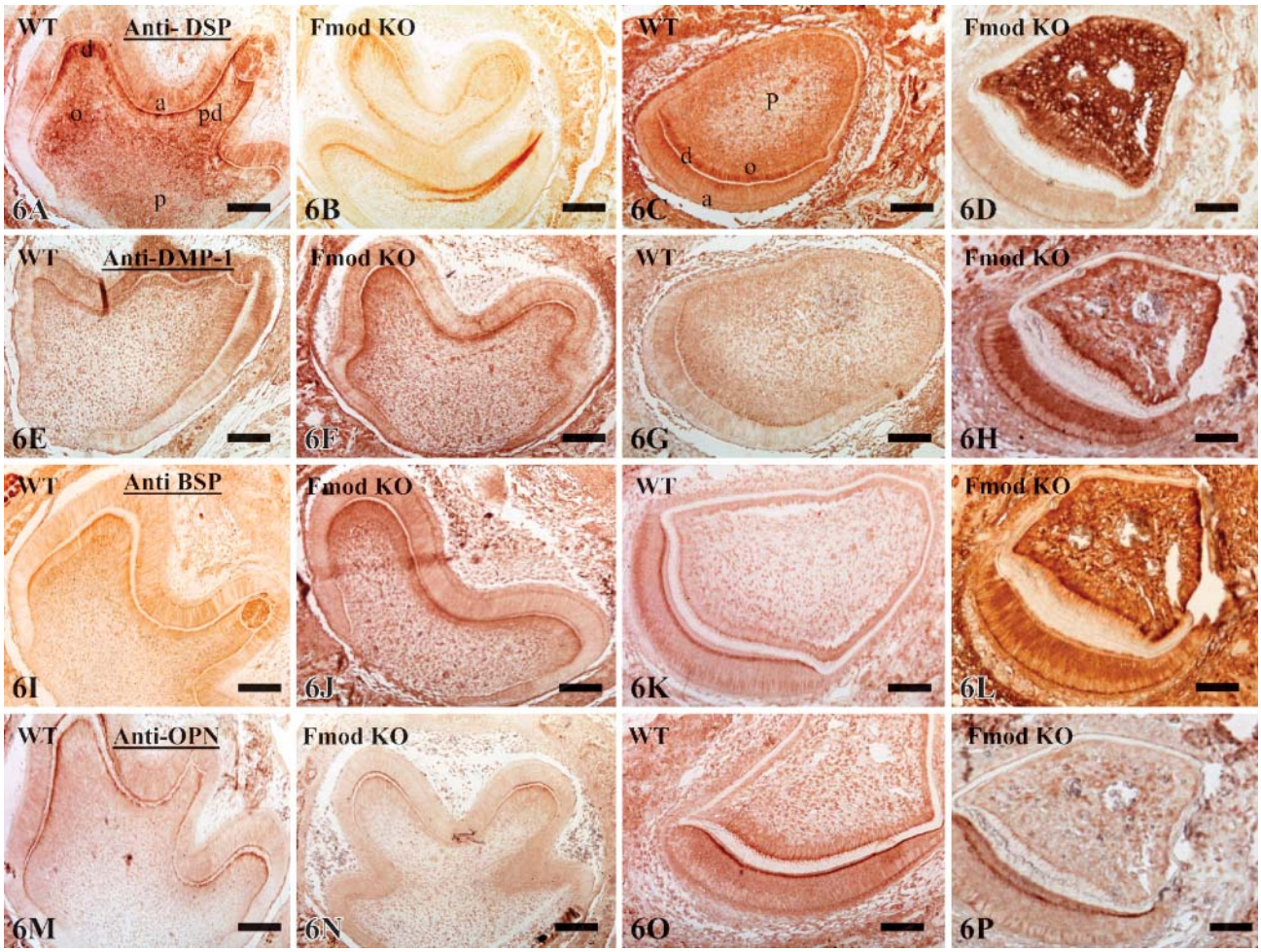

Figure 6 Expression of dentin sialoprotein (DSP) (**A–D**), dental matrix protein 1 (DMP 1) (**E–H**), bone sialoprotein (BSP) (**I–L**), and osteopontin (OPN) (**M–P**) in WT and Fmod KO. (**A,B,E,F,I,J**) In the molars, labeling is reduced for DSP and OPN and enhanced for DMP 1 and BSP. (**C,D,G,H,K,L,O,P**) In contrast, in the incisors the staining for DSP, DMP 1, and BSP is increased in the odontoblast and pulp of Fmod KO incisors compared with WT incisors (compare **D,H,L** to **C,G,K**, respectively). An increased positive staining is found in secretory ameloblasts but only for DMP 1 and BSP. On the opposite, as was the case in the molars, OPN staining is decreased in Fmod KO incisors compared with WT (compare **P** and **O**). Bar = 100 μm.

tent, by ameloblasts, suggesting that Fmod plays a role in odontogenesis. To the best of our knowledge, this is the first report establishing a specific major labeling for Fmod in the SI and along the distal border of secretory odontoblasts where the terminal junctional complex is located (Ushiyama 1989).

Collagen Fibrillogenesis

As no Fmod labeling was detected after light microscope immunostaining, we carried out an electron-immunogold labeling in the forming rat incisor, a method that allows a precise quantitative approach. With respect to the intracellular labeling, the highest values were scored inside odontoblast and ameloblast cell bodies. Compared with the number of antibody–gold complexes counted in the cell bodies, the number of these complexes in the cell processes was half. In the extracellular matrix in dentin and predentin, labeling was weaker than in the cells but nevertheless clearly well above the background levels. Therefore, the present data demonstrate that Fmod is an actual component of predentin and, in consequence, a valid candidate to play a role in collagen fibrillogenesis.

Because SLRPs are known to control collagen fibrillogenesis in various tissues (Vogel and Trotter 1987; Scott and Parry 1992; Scott 1996; Milan et al. 2005), we carefully evaluated the impact of Fmod deficiency on collagen fibrillogenesis. To do so, we specifically focused our attention on the predentin/dentin compartment. This compartment has been extensively used as a model to study the mineralization of collagen matrices because it offers several advantages. First, secretion of collagen in this model is polarized, making

Table 4 Density of the staining obtained with four SIBLINGs (DSP, DMP 1, BSP, and OPN) in four different compartments (ameloblast cell bodies, Am; odontoblast cell bodies, Od; the subodontoblastic area, Sub-od; and pulp, P) of WT and Fmod-deficient molars and incisors[a]

	Molar WT	Molar Fmod-deficient	Incisor WT	Incisor Fmod-deficient
DSP	Am ±	Am –	Am +	Am –
	Od +++ (distal border)	Od ++ (distal border)	Od ++ (distal border)	Od ++
	Sub-od ++	Sub-od –	Sub-od +	Sub-od ++
	Pulp +	Pulp –	Pulp –	Pulp +++
DMP 1	Am +	Am –	Am –	Am ++
	Od ± (distal border)	Od ++ (distal border)	Od +	Od +++
	Sub-od –	Sub-od ±	Sub-od ±	Sub-od ++
	Pulp –	Pulp –	Pulp –	Pulp ++
BSP	Am –	Am +	Am +	Am ++
	Od ± (distal border)	Od ++	Od +	Od +++
	Sub-od –	Sub-od +	Sub-od –	Sub-od ++
	Pulp –	Pulp ±	Pulp –	Pulp ++
OPN	Am ++ (distal border)	Am –	Am + (distal border ++)	Am ± (distal border ++)
	Od ++ (distal border)	Od + (reduced to tip of cusps)	Od + (distal border ++)	Od –
	Sub-od –	Sub-od –	Sub-od –	Sub-od –
	Pulp –	Pulp –	Pulp –	Pulp ±

[a]In the molars of Fmod-deficient mice compared with WT mice, staining is decreased for DSP and OPN. Labeling is increased for DMP 1 and BSP in the odontoblasts and subodontoblastic layers. In the molar, staining is enhanced in Fmod-deficient mice in the odontoblasts and pulp for DSP, DMP 1, and BSP and reduced for OPN.

it simpler to follow the different steps of fibrillogenesis. Native fibrils are secreted in the proximal zone of predentin. From there, they progressively grow throughout predentin before reaching the distal zone where the large fibrils reach their final diameter just before the onset of dentin mineralization (Weinstock and Leblond 1974; Goldberg et al. 1987; Beniash et al. 2000). Second, mineralization occurs rapidly allowing an overview of the whole mineralization process on a single section. Third, dentin is a simpler tissue than bone because dentin, unlike bone, is not remodeled.

Using this model, our present results clearly indicate that the average diameter of the collagen fibrils is increased in predentin in absence of Fmod compared with WT, contrasting with the decrease in diameter found in Fmod-deficient tendon and sclera (Ezura et al. 2000; Ameye et al. 2002; Chakravarti et al. 2003). This discrepancy could be explained by the different ages of the tissues used in these studies. Structural abnormalities of collagen fibrils are progressively acquired with maturation (Svensson et al. 1999; Ameye et al. 2002), and such maturation of the collagen network does not take place in predentin. Indeed, radiolabeling studies have demonstrated that all newly formed collagen fibrils are incorporated in the mineralized tissue within 24 hr after secretion, preventing any aging/maturation of the collagen network (Weinstock and Leblond 1974; Goldberg et al. 1987). Thus, during odontogenesis, Fmod deficiency, like biglycan deficiency but unlike decorin deficiency (Goldberg et al. 2005), promotes the formation of larger collagen fibrils compared with WT. This indicates that during odontogenesis, both biglycan and Fmod control the lateral fusion of collagen fibrils by inhibiting collagen fibrillogenesis in predentin. Because gradients of expression of various extracellular components are known to occur within predentin (Septier et al. 1998,2001; Hall et al. 1999), we compared the expression levels of Fmod between the proximal, central, and distal parts of predentin in the rat incisor (Table 2). Our observations show that Fmod distribution in predentin is constant, a finding identical to what has been reported for biglycan (Septier et al. 2001). Thus, in predentin during odontogenesis, biglycan and Fmod share not only the same function but also the same pattern of distribution. Their homogeneous distribution in predentin suggests that they inhibit the lateral fusion of collagen fibrils during the entire process of fibrillogenesis. Whereas Fmod displays a homogeneous distribution in predentin, we have previously shown that KS and lumican are distributed according to an increasing gradient from the proximal part of predentin toward the distal mineralization front. Despite 48% protein sequence identity and binding to the same region on collagen type I fibrils (Svensson et al. 2000), Fmod and lumican thus have different patterns of distribution in predentin, suggesting that they could play a different role in collagen fibrillogenesis as shown previously in developing mouse tendons (Ezura et al. 2000). That two closely related SLRPs display different functions and patterns of distribution in the same tissue is not really surprising, as other differences between SLRPs have been reported previously. For example, the two class I SLRPs, decorin and biglycan, which display ~57% identity, are also differently distributed in predentin (Septier et al. 2001), and their deficiency produces a different degree of severity in dentin hypomineralization (Goldberg et al. 2002,2005).

Hypomineralization of the Fmod-deficient dentin may be indirectly mediated by the effects of the Fmod deficiency on collagen fibrillogenesis. It is indeed possible that the absence of Fmod, by affecting collagen fibrillogenesis, somehow also affects the spatial distribution or structure of the nucleation sites and, hence, the mineralization of the whole tissue. Alternatively, Fmod could be more directly involved in the mineralization of the collagen matrices. Indeed, Fmod is preferentially localized in the collagen hole zones (Hedlund et al. 1994) where, as demonstrated by electron microscopic tomography reconstructions, crystal first forms during mineralization (Landis et al. 1993). More experiments are clearly needed to better understand the functional role of Fmod in mineralization.

In conclusion to this part of the discussion, the phenotypical characterization of Fmod-deficient teeth indicates that Fmod controls tooth formation by restricting collagen fibrillogenesis in predentin and by promoting dentin mineralization and enamel formation. Together with our previous studies (Goldberg et al. 2005), this paper indicates that the three SLRPs investigated so far in dental tissues, biglycan, decorin, and Fmod, each play a distinct role during odontogenesis even if they also display partial functional overlap with each other. In summary, all three proteoglycans promote dentin mineralization, although only biglycan and Fmod regulate collagen fibrillogenesis in dentinogenesis. If in dentinogenesis both Fmod and biglycan restrict collagen fibrillogenesis and promote dentin mineralization, in contrast, at early stages of amelogenesis Fmod promotes enamel formation when biglycan represses it. Biglycan and Fmod thus have a broader regulatory function in odontogenesis than decorin as they both affect dentinogenesis and amelogenesis, whereas decorin does not seem to directly affect amelogenesis. If a comprehensive understanding of odontogenesis remains elusive, this report constitutes a further step toward a better understanding of the molecular pathways and processes involved in tooth morphogenesis and in the formation and mineralization of collagen matrices.

Compensatory Mechanisms

The similar patterns of distribution of biglycan and Fmod in WT predentin and the identical collagen phenotypes observed in their absence raised the interesting possibility that biglycan could be overexpressed in Fmod-deficient mice to partly compensate the functional impairment resulting from the absence of Fmod. However, we did not find any evidence of such compensatory mechanisms between Fmod and biglycan (or between Fmod and decorin) by light immunohistochemistry. Similarly, amelogenin was not overexpressed in absence of Fmod contrary to what has been reported in the absence of biglycan (Goldberg et al. 2005).

Compensatory mechanisms involving the SIBLING family were found in the teeth of Fmod-deficient mice. In the molar, staining was slightly decreased for DSP and OPN, whereas DMP 1 and BSP were increased in the odontoblast layer alone, the staining of the rest of the section being unchanged. In contrast, in the incisor, DSP, DMP 1, and BSP were overexpressed in the Fmod-deficient mice, mainly in the odontoblasts but also in the pulp, which normally do not express these molecules as shown by the lack of staining of WT sections. In addition, DMP 1 and BSP were strongly positive in the secretory ameloblasts in Fmod-deficient incisors, whereas the staining was very weak or nil for OPN.

Hence, the absence of Fmod, in a significant manner, modifies extensively the composition of the incisors, whereas the deficiency has a lesser impact on the molars. Whether this is correlated to the fact that incisors, unlike molars, are continuously growing teeth is currently unknown. Although the outcome of the dramatic increase in expression of several SIBLINGs is unknown, it is interesting to speculate about possible consequences.

Because SIBLINGs were first discovered in mineralized tissues including dentin and bone, they were originally believed to be associated with the mineralization processes (for review, see Goldberg et al. 1995; Qin et al. 2004). Consequently, it was hypothesized that increased levels of SIBLINGs should result in increased mineralization. However, this was not the case (Qin et al. 2004). The fact that they also have been recently identified in non-mineralized tissues such as liver, brain, pancreas, salivary glands, cancers, and kidney modifies the original view and suggests that SIBLINGs have additional functions (Fisher et al. 2004; Ogbureke and Fisher 2004,2005; Terasawa et al. 2004).

With respect to the role of SIBLINGs in the mineralization processes, in vivo and in vitro data are conflicting. Although there is a general belief that SIBLINGs are implicated in dental and bone mineralization, it appears that DSP has limited effects on in vitro apatite formation and growth (Boskey et al. 2000). In a gelatin gel-diffusion system, OPN and BSP are inhibitors of calcium phosphate nucleation and growth (Boskey 1995; Boskey et al. 2000). In its native form, DMP 1 inhibits mineralization, but when cleaved or dephosphorylated it initiates mineralization (Tartaix et al. 2004). Proteolytic processing of DMP 1 catalyzed by the BMP 1/Tolloid-like proteinases plays a crucial role during osteogenesis and probably dentinogenesis (Steiglitz et al. 2004). Our results clearly show that the absence of Fmod induces changes in the protein levels of several SIBLINGs, but the performed immunohistochemical stainings do not allow us to detect or to quantify the diverse modifications (phosphorylation, deglycosylation, degradation) that the SIBLINGs may undergo (Boskey et al. 1990; Gericke et al. 2005). Hence, in the absence of any data regarding the different forms of SIBLINGs, and in view

of the opposite functions that different forms of the same SIBLING may have, it is currently difficult to interpret what the functional consequences of the differential expressions of the SIBLINGs observed in the Fmod-deficient tissues could be.

New functions have been reported for SIBLINGs. It is now well documented that phosphophoryn (DPP) regulates the gene expression and differentiation of some osteoblast cell lines and adult mesenchymal stem cells. This suggests that DPP possesses signaling functions implicated in cell differentiation (Jadlowiec et al. 2004). Dual functions or multifunctional properties are also apparently the case for DMP 1, an extracellular matrix component implicated in dentin mineralization (Ye et al. 2004) but also in the differentiation of odontoblasts and osteoblasts (Narayanan et al. 2001,2004). Together these data underscore the importance of having an extracellular matrix with a balanced composition to control not only the structure but also the function of mineralizing tissues. The fact that DSP and DMP 1 are detected both in presecretory ameloblasts and ameloblasts at an early stage of secretion, as well as odontoblasts, suggests that these molecules are implicated mostly in cell differentiation and other developmental regulation rather than in the mineralization of a matrix which has not yet been secreted (MacDougall et al. 1998).

To the best of our knowledge, previously unsuspected compensatory mechanisms between Fmod and SIBLINGs are reported here for the first time. The coupled upregulation of DMP 1 and BSP in Fmod-deficient molars and incisors suggests that a functional link may exist between the two molecules. In contrast, DSP and OPN are downregulated in the molar but display diverging changes in protein expression in the incisor. In addition, changes in collagen fibrillogenesis could be due, in part, to the changes in those molecules, as some of them are known to bind collagen. The subtle balance between molecules that are specifically upregulated or downregulated following various conditions such as gene deletion open fascinating new areas of research.

Acknowledgments

We thank the Institut Benjamin Delessert for financial support for this study. Part of this work was supported by the Intramural Program of the National Institute of Dental and Craniofacial Research (NIDCR), National Institutes of Health, Bethesda, MD.

Literature Cited

Ameye L, Aria D, Jepsen K, Oldberg A, Xu T, Young MF (2002) Abnormal collagen fibrils in tendons of biglycan/fibromodulin-deficient mice lead to gait impairment, ectopic ossification, and osteoarthritis. FASEB J 16:673–680

Beniash E, Traub W, Veis A, Weiner S (2000) A transmission electron microscope study using vitrified ice sections of predentin: structural changes in the dentin collagenous matrix prior to mineralization. J Struct Biol 132:212–225

Boskey AL (1995) Osteopontin and related phosphorylated sialoproteins: effects on mineralization. Ann N Y Acad Sci 21:249–256

Boskey AL, Muresca S, Doty S, Sabsay B, Veis A (1990) Concentration dependent effects of dentin phosphoryn in the regulation of in vitro hydroxyapatite formation and growth. Bone Miner 11:55–65

Boskey A, Spevak L, Tan M, Doty SB, Butler WT (2000) Dentin sialoprotein (DSP) has limited effects on in vitro apatite formation and growth. Calcif Tissue Int 67:472–478

Buchaille R, Couble ML, Magloire H, Bleicher F (2000) Expression of the small leucine-rich proteoglycan osteoadherin/osteomodulin in human dental pulp and developing rat teeth. Bone 27:265–270

Chakravarti S, Paul J, Roberts L, Chervoneva I, Oldberg A, Birk DE (2003) Ocular and scleral alterations in gene-targeted lumican-fibromodulin double-null mice. Invest Ophthalmol Vis Sci 44: 2422–2432

Embery G, Hall R, Waddington R, Septier D, Goldberg M (2001) Proteoglycans in dentinogenesis. Crit Rev Oral Biol Med 12:331–349

Ezura Y, Chakravarti S, Oldberg A, Chervoneva I, Birk DE (2000) Differential expression of lumican and fibromodulin regulate collagen fibrillogenesis in developing mouse tendons. J Cell Biol 151:779–788

Fisher LW, Fedarko NS (2003) Six genes expressed in bones and teeth encode the current members of the SIBLING family of proteins. Connect Tissue Res 44:33–40

Fisher LW, Jain A, Tayback M, Fedarko NS (2004) Small integrin binding ligand N-linked glycoprotein gene family expression in different cancers. Clin Cancer Res 15:8501–8511

Fisher LW, Stubbs JT III, Young MF (1995) Antisera and cDNA probes to human and certain animal model bone matrix noncollagenous proteins. Acta Orthop Scand 266:61–65

Font B, Eichenberger D, Goldschmidt D, Boutillon MM, Hulmes DJ (1998) Structural requirements for fibromodulin binding to collagen and the control of type I collagen fibrillogenesis-critical roles for disulphide bonding and the C-terminal region. Eur J Biochem 254:580–587

Gericke A, Qin C, Spevak L, Fujimoto Y, Butler WT, Sorensen ES, Boskey AL (2005) Importance of phosphorylation for osteopontin regulation of biomineralization. Calcif Tissue Int 77:45–54

Goldberg M, Rapoport O, Septier D, Palmier K, Hall R, Embery G, Young M, et al. (2003) Proteoglycans in predentin: the last 15 micrometers before mineralization. Connect Tissue Res 44:184–188

Goldberg M, Septier D (1996) A comparative study of the transition between predentin and dentin, using various preparative procedures in the rat. Eur J Oral Sci 104:269–277

Goldberg M, Septier D, Escaig-Haye F (1987) Glycoconjugates in dentinogenesis and dentine. Prog Histochem Cytochem 17:1–112

Goldberg M, Septier D, Lécolle S, Chardin H, Quintana MA, Acevedo AC, Gafni G, et al. (1995) Dental mineralization. Int J Dev Biol 39:93–110

Goldberg M, Septier D, Rapoport O, Iozzo RV, Young MF, Ameye LG (2005) Targeted disruption of two small leucine-rich proteoglycans, biglycan and decorin, excerpts divergent effects on enamel and dentin formation. Calcif Tissue Int 77:297–310

Goldberg M, Septier D, Rapoport O, Young M, Ameye L (2002) Biglycan is a repressor of amelogenin expression and enamel formation: an emerging hypothesis. J Dent Res 81:520–524

Goldberg M, Takagi M (1993) Dentine proteoglycans: composition, ultrastructure and functions. Histochem J 25:781–806

Hall R, Septier D, Embery G, Goldberg M (1999) Stromelysin-1 (MMP-3) in forming enamel and predentine in rat incisor-coordinated distribution with proteoglycans suggests a functional role. Histochem J 31:761–770

Hedlund H, Mengarelli-Widholm S, Heinegard D, Reinholt FP, Svensson O (1994) Fibromodulin distribution and association with collagen. Matrix Biol 14:227–232

Iozzo RV (1997) The family of the small leucine-rich proteoglycans: key regulators of matrix assembly and cellular growth. Crit Rev Biochem Mol Biol 32:141–174

Iozzo RV (1999) The biology of the small leucine-rich proteoglycans.

Functional network of interactive proteins. J Biol Chem 274: 18843–18846
Jadlowiec J, Koch H, Zhang X, Campbell PG, Seydain M, Sfeir C (2004) Phosphoryn regulates the gene expression and differentiation of NIH3T3, MC3T3–E1, and human mesenchymal stem cells via the integrin/MAPK signaling pathway. J Biol Chem 279: 53323–53330
Landis WJ, Song MJ, Leith A, McEwen L, McEwen BF (1993) Mineral and organic matrix interaction in normally calcifying tendon visualized in three dimensions by high-voltage electron microscopic tomography and graphic image reconstruction. J Struct Biol 110:39–54
Linde A, Goldberg M (1993) Dentinogenesis. Crit Rev Oral Biol Med 4:679–728
Lormée P, Septier D, Lecolle S, Baudoin C, Goldberg M (1996) Dual incorporation of (35S)sulfate into dentin proteoglycans acting as mineralization promotors in rat molars and predentin proteoglycans. Calcif Tissue Int 58:368–375
MacDougall M, Nydegger J, Gu TT, Simmons D, Luan X, Cavender A, D'Souza RN (1998) Developmental regulation of dentin sialophosphoprotein during ameloblast differentiation: a potential enamel matrix nucleator. Connect Tissue Res 39:25–37
Matheson S, Larjava H, Hakkinen L (2005) Distinctive localization and function for lumican, fibromodulin and decorin to regulate collagen fibril organization in periodontal tissues. J Periodontal Res 40:312–324
Milan AM, Sugars RV, Embery G, Waddington RJ (2005) Modulation of collagen fibrillogenesis by dentinal proteoglycans. Calcif Tissue Int 76:127–135
Narayanan K, Srinivas R, Peterson MC, Ramachandran A, Hao J, Thimmapaya B, Scherer PE, et al. (2004) Transcriptional regulation of dentin matrix protein 1 by JunB and p300 during osteoblast differentiation. J Biol Chem 279:44294–44302
Narayanan K, Srinivas R, Ramachandran A, Hao J, Quinn B, George A (2001) Differentiation of embryonic mesenchymal cells to odontoblast-like cells by overexpression of dentin matrix protein 1. Proc Natl Acad Sci USA 98:4516–4521
Neame PJ, Kay CJ (2000) Small Leucin-rich proteoglycans. In RV Iozzo, ed. Proteoglycans—Structure, Biology and Molecular Interactions. New York, Marcel Dekker, 201–235
Ogbureke KU, Fisher LW (2004) Expression of SIBLINGs and their partner MMPs in salivary glands. J Dent Res 83:664–670
Ogbureke KU, Fisher LW (2005) Renal expression of SIBLING proteins and their partner matrix metalloproteinases (MMPs). Kidney Int 68:155–166
Oldberg A, Antonsson P, Lindblom K, Heinegard D (1989) A collagen-binding 59-kd protein (fibromodulin) is structurally related to the small interstitial proteoglycans PG-S1 and PG-S2 (decorin). EMBO J 8:2601–2604
Qin C, Baba O, Butler WT (2004) Post-translational modifications of sibling proteins and their roles in osteogenesis and dentinogenesis. Crit Rev Oral Biol Med 15:126–136
Scott JE (1988) Proteoglycan-fibrillar collagen interactions. Biochem J 252:313–323
Scott JE (1996) Proteodermatan and proteokeratan sulfate (decorin, lumican/fibromodulin) proteins are horseshoe shaped. Implications for their interactions with collagen. Biochemistry 35:8795–8799
Scott JE, Parry DA (1992) Control of collagen fibril diameters in tissues. Int J Biol Macromol 14:292–293
Septier D, Hall RC, Embery G, Goldberg M (2001) Immunoelectron microscopic visualization of pro- and secreted forms of decorin and biglycan in the predentin and during dentin formation in the rat incisor. Calcif Tissue Int 69:38–45
Septier D, Hall RC, Lloyd D, Embery G, Goldberg M (1998) Quantitative immunohistochemical evidence of a functional gradient of chondroitin 4-sulphate/dermatan sulphate, developmentallyregulated in the predentine of rat incisor. Histochem J 30: 12275–284
Soo C, Hu FY, Zhang X, Wang Y, Beanes SR, Lorenz HP, Hedrick MH, et al. (2000) Differential expression of fibromodulin, a transforming growth factor-beta modulator, in fetal skin development and scarless repair. Am J Pathol 157:423–433
Steiglitz BM, Avala M, Narayanan K, George A, Greenspan DS (2004) Bone morphogenetic protein-1/Tolloid-like proteinases process dentin matrix protein-1. J Biol Chem 279:980–986
Steinfort J, van de Stadt R, Beertsen W (1994) Identification of new rat dentin proteoglycans utilizing C18 chromatography. J Biol Chem 269:22397–22404
Svensson L, Aszodi A, Reinholt FP, Fassler R, Heinegard D, Oldberg A (1999) Fibromodulin-null mice have abnormal collagen fibrils, tissue organization, and altered lumican deposition in tendon. J Biol Chem 274:9636–9647
Svensson L, Narlid I, Oldberg A (2000) Fibromodulin and lumican bind to the same region on collagen type I fibrils. FEBS Lett 470: 178–182
Takagi M, Hishikawa H, Hosokawa Y, Kagami A, Rahemtulla F (1990) Immunohistochemical localization of glycosaminoglycans and proteoglycans in predentin and dentin of rat incisors. J Histochem Cytochem 38:319–324
Tartaix PH, Doulaverakis M, George A, Fisher LW, Butler WT, Qin C, Salih E, et al. (2004) In vitro effects of dentin matrix protein-1 on hydroxyapatite formation provide insights into in vivo functions. J Biol Chem 279:18115–18120
Terasawa M, Shimokawa R, Terashima T, Ohya K, Takagi Y, Shimokawa H (2004) Expression of dentin matrix protein 1 (DMP1) in nonmineralized tissues. J Bone Miner Metab 22:430–438
Ushiyama J (1989) Gap junctions between odontoblasts revealed by transjunctional flux of fluorescent tracers. Cell Tissue Res 258:611–616
Vogel KG, Trotter JA (1987) The effect of proteoglycans on the morphology of collagen fibrils formed in vitro. Coll Relat Res 7:105–114
Weinstock M, Leblond CP (1974) Synthesis, migration, and release of precursor collagen by odontoblasts as visualized by radioautography after (3H)proline administration. J Cell Biol 60:92–127
Wilda M, Bachner D, Just W, Geerkens C, Kraus P, Vogel W, Hameister H (2000) A comparison of the expression pattern of five genes of the family of small leucine-rich proteoglycans during mouse development. J Bone Miner Res 15:2187–2196
Ye L, MacDougall M, Zhang S, Xie Y, Zhang J, Li Z, Lu Y, et al. (2004) Deletion of Dentin Matrix Protein-1 leads to a partial failure of maturation of predentin into dentin, hypomineralization, and expanded cavities of pulp and root canal during postnatal tooth development. J Biol Chem 279:19141–19148

The Journal of Histochemistry & Cytochemistry